Tricritical behavior of the Blume-Capel model*

D. M. Saul and Michael Wortis
Physics Department, University of Illinois, Urbana, Illinois 61801

D. Stauffer
Physik-Department T30, 8046 Garching, Reaktorgelaende, West Germany
(Received 28 December 1973)

The thermodynamic behavior of the fcc Blume-Capel ferromagnet,

$$\mathcal{H} = -J\sum_{\langle 12\rangle} S^z(1)S^z(2) + \Delta\sum_1 [S^z(1)]^2 - h\sum_1 S^z(1), \quad S^z = 0, \pm 1,$$

is studied by series-extrapolation techniques. By using both high- and low-temperature series, we are able to trace first- and second-order branches of the phase boundary and examine behavior at temperatures both above and below the phase transition. We find a tricritical point at $k_BT_t/12J = 0.2615 \pm 0.0070$, $\Delta_t/12J = 0.4716 \pm 0.0010$. Tricritical exponents are consistent with $\gamma_t = \gamma_t' = 1$, $\beta_t = 1/4$, $\varphi_t = \nu_t = \alpha_t = \alpha_t' = 1/2$, in good agreement with tricritical mean-field theory and the Gaussian tricritical fixed point of Riedel and Wegner.

I. INTRODUCTION

Griffiths[1] first pointed out indications of special, characteristic tricritical behavior with particular reference to He^3-He^4 mixtures.[2] The He^3-He^4 tricritical point (TCP) has by now been studied in some detail.[3,4] Analogous behavior has been seen in a variety of other systems, including the structural transition of NH_4Cl[5] and the metamagnetic transitions of dysprosium aluminum garnet (DAG)[6-8] and $FeCl_2$.[9,10]

On the theoretical side, Riedel[11] and later Hankey *et al.*[12] and Griffiths[13] showed how to introduce "scaling fields" to give a unified semiphenomenological description of the first- and second-order regions, the tricritical region, and the crossover between them. The values of the tricritical exponents and the shape of the scaling function are left open by the semiphenomenological scaling theory. Tricritical mean-field theory[1,14] supplies both but is suspect, since it neglects fluctuations. However, Riedel and Wegner,[15,16] using renormalization-group techniques to include the effect of fluctuations, discovered a Gaussian tricritical fixed point in three dimensions ($d = 3$) exhibiting mean-field exponents modified by logarithmic corrections.[17] (Very recently Riedel and Wegner[18] have studied the detailed structure of the scaling function.) Bausch[19] showed that the special status of the $d = 3$ tricritical point could be understood by applying the Ginzburg criterion[20]: Close enough to the TCP fluctuation effects dominate for $d < 3$ but are negligible for $d > 3$ (so mean-field theory is applicable). The borderline $d = 3$ ($d = 4$ is the analogous dimension for critical phenomena) is characterized by logarithmic corrections.[17]

He^3-He^4 seems to fit well into the Riedel-Wegner pattern. Data for NH_4Cl, DAG, and $FeCl_2$ are more tentative but, as of this writing, they appear to show departures from mean-field exponents. For further exploration, then, one turns to models, the study of which is free of various experimental difficulties (though it has, as we shall see, special problems of its own).

The model we work with is a special case ($K = 0$) of the so-called Blume-Emery-Griffiths (BEG) model,[14] originally introduced independently by Blume[21] and Capel[22] in quite other contexts. It is an $s = 1$ lattice model defined by the Hamiltonian

$$\mathcal{H} = -J\sum_{\langle 12\rangle} S^z(1)S^z(2) + \Delta\sum_1 [S^z(1)]^2 - h\sum_1 S^z(1), \quad S^z = 0, \pm 1. \tag{1.1}$$

The interaction J is greater than zero and the first sum is over nearest-neighbor pairs $\langle 12\rangle$. h is the magnetic field. For $\Delta = -\infty$ the $S^z = 0$ state is suppressed, and the Blume-Capel model reduces to the $s = \frac{1}{2}$ Ising model. For $\Delta = 0$, it is just the $s = 1$ Ising model. At $\Delta = +\infty$ the $S^z = \pm 1$ states are suppressed, and the model is paramagnetic at all temperatures. BEG[14] showed that the $h = 0$ magnetic-ordering temperature goes to zero when $\Delta/qJ = \frac{1}{2}$ (an exact result), where q is the coordination number of the lattice. They calculated the full phase diagram *in mean-field theory* (see our Figs. 2–4) and found that the $h = 0$ transition remains second order up to a tricritical point[23] at $\Delta/qJ = \frac{2}{3}\ln 2$ ($k_BT/qJ = \frac{1}{3}$), where it abruptly turns first order.

In this paper we perform a complete, detailed analysis of the tricritical behavior of the fcc Blume-Capel model (1.1) *beyond* the mean-field approximation by the use of high- and low-temperature series expansions. Preliminary results have been reported previously.[24] Earlier high-tempera-

ture work has been reported by Oitmaa,[25-27] using series shorter than ours. The second-order region of his phase diagram is in general agreement with ours (Sec. III A); however, lacking low-temperature series, he has no data in the first-order region, was unable to locate the TCP with any precision, and could not explore tricritical behavior. Arora and Landau[28] have reported Monte Carlo results for the $d=2$ Blume-Capel model (see Sec. V) and are presently using[29] similar techniques to investigate the fcc lattice. Finally, we note that Harbus and Stanley[30,31] have done some high-temperature-series work on two $d=3$ lattice models more or less related to the Blume-Capel model (see Sec. V).

Our plan of exposition is as follows: Section II discusses the derivation of high- and low-temperature series (see Tables I and II) and their analysis. It can be omitted by the reader interested in results only. Section III presents the mapping out of the phase diagram, with particular emphasis on the techniques for finding the first-order part of the phase boundary and locating the TCP. These results are contained in Figs. 2–6. Section IV is devoted to the determination of tricritical exponents and amplitudes. Some principal results are summarized in Tables III and IV. In Sec. V we briefly recapitulate important points and compare our results with other work. The principal conclusion of this study is that the tricritical behavior of the $d=3$ Blume-Capel model is consistent with the mean-field, Riedel-Wegner, Gaussian-tricritical-fixed-point picture.

II. SERIES EXPANSIONS

A. Derivation of high-temperature-series coefficients

High-temperature series for the thermodynamic functions of the Blume-Capel model (1.1) take the form $\sum_{n=0}^{\infty} c_n(\beta\Delta, \beta h)(\beta J)^n$. The linked-cluster expansion[32-34] provides a prescription for writing down the coefficients c_n as sums of products of so-called "bare semi-invariants," M_k^0. The $h=0$ semi-invariants $M_k^0(\beta\Delta)$ are related to the noninteracting ($J=0$) Helmholtz free energy per spin,

$$-\beta f(\beta J=0, \beta\Delta, \beta h) = \ln \sum_{s=-1}^{1} e^{-\beta\Delta s^2+\beta h s}$$

$$= -\ln(1-\tau) + \ln[1+\tau(\cosh\beta h - 1)]$$

$$= \sum_{n=0}^{\infty} \frac{M_n^0(\beta\Delta)(\beta h)^n}{n!}, \tag{2.1}$$

where

$$0 \le \tau \equiv (1+\tfrac{1}{2}e^{\beta\Delta})^{-1} \le 1. \tag{2.2}$$

f is even in h, so the odd semi-invariants vanish at $h=0$. The even M_k^0's satisfy the recursion relation[35]

$$M_{2n}^0 = \tau\left[1 - \frac{(2n)!}{n}\sum_{l=1}^{n-1} \frac{l M_{2l}^0}{(2n-2l)!(2l)!}\right], \quad n>0,$$

so $M_2^0=\tau$, $M_4^0=\tau-3\tau^2$, etc., and, in general, M_{2n}^0 is a polynomial in τ with no constant term and maximum order τ^n. It follows that the coefficients c_n are also polynomials in τ, and we are now in a position to calculate the minimum and maximum powers of τ which occur.

Consider the free energy per spin[36]

$$-\beta f(\beta J, \beta\Delta, \beta h) \equiv \ln \mathrm{Tr} e^{-\beta\mathcal{H}}/N. \tag{2.3}$$

At $h=0$,

$$-\beta f(\beta J, \beta\Delta, 0) = -\ln(1-\tau) + \sum_{n=2}^{\infty} p_n(\tau)(\beta J)^n. \tag{2.4}$$

The linked-cluster graphs contributing to the polynomial $p_n(\tau)$ are connected graphs with n edges and no odd vertices. Each vertex with l incident edges carries a factor M_l^0. Since there are a total of $2n$ bond ends, the maximum power of τ in $p_n(\tau)$ is τ^n. The minimum power of τ comes from the graph with the smallest number of vertices, which gives τ^2 (n even) or τ^3 (n odd) and, in fact,[37]

$$p_n(\tau) = \sum_{l=2}^{n} p_{nm}\tau^m, \quad p_{n2} = \begin{cases} q/2n!, & n \text{ even} \\ 0 & n \text{ odd}, \end{cases} \tag{2.5}$$

where q is the coordination number of the lattice. The expansions corresponding to (2.4) for the zero-field susceptibility and second spherical moment of correlations are

$$k_B T \chi_0 = -k_B T \left.\frac{\partial^2 f}{\partial h^2}\right|_{h=0} = \sum_{\vec{r}} \langle S(\vec{r})\, S(\vec{0})\rangle$$

$$= \tau + \sum_{n=1}^{\infty} m_n^{(0)}(\tau)(\beta J)^n \tag{2.6}$$

and

$$\mu_2 = \sum_{\vec{r}} \left(\frac{r}{a}\right)^2 \langle S(\vec{r})\, S(\vec{0})\rangle = \sum_{n=1}^{\infty} m_n^{(2)}(\tau)(\beta J)^n, \tag{2.7}$$

where a is the nearest-neighbor lattice distance.

It is not hard to show that the polynomials

$$L_n \equiv n!\, p_n(\tau)/6, \quad H_n \equiv n!\, m_n^{(0)}(\tau)/12,$$

and

$$S_n \equiv n!\, m_n^{(2)}(\tau)/12 \tag{2.8}$$

have integer coefficients. Oitmaa[25-27] has calculated L_n and H_n through orders 9 and 7, respectively, by a method rather different from ours. No second-moment polynomials have previously been published. In Table I we present polynomials $L_n(10 \le n \le 13)$, $H_n(8 \le n \le 12)$, and $S_n(1 \le n \le 12)$ for the fcc lattice.[38] To derive these polynomials we proceeded as follows: Our computer codes[33,39] accept as input numerical values of the semi-invariants M_{2k}^0, $1 \le k \le 6$, and generate high-temperature

TABLE I. High-temperature polynomials. Definitions are given in Eqs. (2.4) and (2.6)–(2.8). Low-order L_n and H_n are given in Refs. 25 and 27. The coefficients quoted as integers are exact; those given as decimal fractions are approximate (see text).

$$L_{10} = \tau^2 + 23\,250\tau^3 + 10\,433\,745\tau^4 + 834\,469\,020\tau^5 + 21\,362\,131\,980\tau^6 + 166\,388\,342\,400\tau^7 + 271\,169\,054\,100\tau^8 + 320\,312\,588\,400\tau^9 + 267\,023\,116\,080\tau^{10}$$

$$L_{11} = 59\,048\tau^3 + 48\,618\,240\tau^4 + 5\,908\,617\,000\tau^5 + 236\,340\,886\,320\tau^6 + 3\,484\,135\,892\,160\tau^7 + 14\,287\,964\,090\,400\tau^8 + 19\,761\,751\,548\,000\tau^9 + 27\,695\,383\,531\,200\tau^{10} + 19\,508\,777\,164\,800\tau^{11}$$

$$L_{12} = \tau^2 + 191\,466\tau^3 + 259\,917\,603\tau^4 + 12!\,(92.749\,131\,444\tau^5 + 5195.317\,582\,1\tau^6 + 115\,517.044\,20\tau^7 + 987\,508.878\,78\tau^8 + 2\,559\,334.3200\tau^9 + 3\,832\,466.5511\tau^{10} + 5\,256\,430.5090\tau^{11} + 3\,354\,721.5596\tau^{12})$$

$$L_{13} = 531\,440\tau^3 + 1\,309\,788\,480\tau^4 + 13!\,(37.641\,591\,677\tau^5 + 4406.406\,064\,6\tau^6 + 123\,206.610\,39\tau^7 + 1\,806\,816.9269\tau^8 + 9\,105\,601.8972\tau^9 + 19\,136\,009.047\tau^{10} + 31\,067\,574.821\tau^{11} + 3\,968\,4236.365\tau^{12} + 2\,3601\,813.178\tau^{13})$$

$$H_8 = \tau^2 + 12\,054\tau^3 + 3\,506\,055\tau^4 + 225\,509\,088\tau^5 + 5\,009\,298\,210\tau^6 + 43\,580\,077\,380\tau^7 + 172\,155\,981\,060\tau^8 + 304\,363\,203\,480\tau^9$$

$$H_9 = \tau^2 + 33\,090\tau^3 + (9!/12)\,(552.828\,548\,10\tau^4 + 53\,377.546\,418\tau^5 + 1\,815\,313.5969\tau^6 + 25\,458\,599.084\tau^7 + 164\,626\,517.98\tau^8 + 544\,943\,773.61\tau^9 + 836\,643\,829.46\tau^{10})$$

$$H_{10} = \tau^2 + 97\,506\tau^3 + (10!/12)\,(269.497\,642\,03\tau^4 + 37\,787.964\,491\tau^5 + 1\,841\,534.9230\tau^6 + 38\,753\,667.478\tau^7 + 383\,025\,259.24\tau^8 + 1\,984\,584\,648.3\tau^9 + 5\,680\,768\,591.1\tau^{10} + 7\,705\,111\,699.5\tau^{11})$$

$$H_{11} = \tau^2 + 280\,038\tau^3 + (11!/12)\,(121.686\,581\,17\tau^4 + 24\,305.733\,138\tau^5 + 1\,643\,194.6805\tau^6 + 48\,535\,982.236\tau^7 + 699\,482\,071.56\tau^8 + 5\,290\,642\,945.6\tau^9 + 23\,062\,573\,672.\tau^{10} + 58\,285\,057\,762.\tau^{11} + 70\,795\,082\,864.\tau^{12})$$

$$H_{12} = \tau^2 + 832\,974\tau^3 + (12!/12)\,(541.893\,079\,21\tau^4 - 2433.192\,302\,6\tau^5 + 1\,578\,958.4475\tau^6 + 50\,461\,532.756\tau^7 + 1\,062\,812\,818.6\tau^8 + 11\,158\,178\,059.\tau^9 + 68\,956\,224\,515.\tau^{10} + 260\,474\,335\,009.\tau^{11} + 590\,481\,944\,720.\tau^{12} + 649\,166\,451\,013.\tau^{13})$$

$$S_1 = \tau^2$$

$$S_2 = 48\tau^3$$

$$S_3 = \tau^2 + 66\tau^3 + 2385\tau^4$$

$$S_4 = 240\tau^3 + 10\,080\tau^4 + 133\,488\tau^5$$

$$S_5 = \tau^2 + 450\tau^3 + 51\,105\tau^4 + 1\,156\,500\tau^5 + 8\,474\,040\tau^6$$

$$S_6 = 1\,368\tau^3 + 203\,040\tau^4 + 9\,176\,040\tau^5 + 124\,582\,320\tau^6 + 606\,201\,840\tau^7$$

$$S_7 = \tau^2 + 3\,066\tau^3 + 923\,685\tau^4 + 59\,855\,040\tau^5 + 1\,477\,543\,410\tau^6 + 13\,532\,339\,520\tau^7 + 48\,427\,921\,710\tau^8$$

$$S_8 = 9120\tau^3 + 3\,890\,880\tau^4 + 396\,956\,448\tau^5 + 14\,392\,990\,080\tau^6 + 226\,409\,924\,160\tau^7 + 1\,525\,900\,481\,280\tau^8 + 4\,281\,839\,755\,200\tau^9$$

$$S_9 = \tau^2 + 23\,250\tau^3 + (9!/12)\,(594.661\,562\,682\,8\tau^4 + 84\,294.383\,697\,93\tau^5 + 4\,410\,909.076\,850\tau^6 + 102\,221\,850.1385\tau^7 + 1\,134\,215\,232.907\tau^8 + 5\,981\,857\,240.675\tau^9 + 13\,743\,018\,904.44\tau^{10})$$

$$S_{10} = 68\,424\tau^3 + (10!/12)\,(270.619\,998\,266\,9\tau^4 + 55\,513.104\,452\,69\tau^5 + 3\,943\,812.967\,795\tau^6 + 127\,739\,737.9327\tau^7 + 2\,066\,854\,791.541\tau^8 + 17\,380\,438\,625.12\tau^9 + 74\,941\,201\,760.29\tau^{10} + 145\,366\,249\,377.3\tau^{11})$$

$$S_{11} = \tau^2 + 191\,466\tau^3 + (11!/12)\,(118.932\,906\,189\,9\tau^4 + 33\,538.292\,855\,22\tau^5 + 3\,197\,620.768\,745\tau^6 + 137\,665\,792.4022\tau^7 + 306\,381\,3085.557\tau^8 + 36\,980\,537\,599.12\tau^9 + 248\,244\,844\,269.4\tau^{10} + 903\,379\,027\,460.2\tau^{11} + 1\,513\,692\,561\,261.\tau^{12})$$

$$S_{12} = 572\,400\tau^3 + (12!/12)\,(761.216\,970\,838\,6\tau^4 - 5702.401\,272\,527\tau^5 + 2\,759\,120.760\,728\tau^6 + 129\,871\,665.2661\tau^7 + 3\,903\,405\,735.617\tau^8 + 63\,590\,860\,590.51\tau^9 + 603\,431\,062\,267.8\tau^{10} + 3\,358\,190\,461\,783.\tau^{11} + 10\,562\,385\,264\,135.\tau^{12} + 15\,559\,184\,767\,727.\tau^{13})$$

series for the zero-field ($h = 0$) correlations $\langle S(\vec{r})S(\vec{0})\rangle$ through 12th order in (βJ) for any Ising-like model on the three cubic lattices. Thus, for a fixed, numerical value of τ we can find numerical values of the coefficients $m_n^{(0)}(\tau)$ and $m_n^{(2)}(\tau)$ via (2.6) and (2.7), and $p_n(\tau)$ via the relation

$$-\beta f(\beta J, \beta\Delta, 0) = -\ln(1-\tau) + \tfrac{1}{2}q\int_0^{\beta J} d(\beta J)\langle S(\vec{\delta})S(\vec{0})\rangle \tag{2.9}$$

where $\vec{\delta}$ is a nearest-neighbor lattice vector. For each set of numerical values $\{\tau, p_n(\tau)\}$, Eq. (2.5) (and the corresponding equations for $m_n^{(0)}$ and $m_n^{(2)}$) becomes a linear relation for the unknown polynomial coefficients p_{nm}. Numerical data for $n-2$ different τ's determine the full polynomial $p_n(\tau)$. In practice we have calculated p_{n3} and p_{n4} exactly,[40] thus providing a check and reducing the number of necessary data sets to $n-4$.

The numbers quoted as integers in Table I are exact. Those given as decimal fractions are only approximate: Because of rounding errors, the original computer output $p_n(\tau)$ has only about 12–13 significant figures in higher orders. Further significance is lost in matrix inversion. Integer precision in L_n requires that the p_{nm}'s emerging from the matrix inversion have enough decimal places to identify the decimal fraction. In addition, the graphs contributing in order n range in value from roughly q^n to $q/n!$ and, when the ratio exceeds 10^{12-13}, coefficients of the smaller graphs become entirely lost in the noise. Thus, the decimal coefficients in lower orders are good approximations, but the smaller coefficients lose significance as n increases. Finally, the highest order in our program may[41] have a small error, so the decimal coefficients in L_{13}, H_{12}, and S_{12} are approximate at best, an effect exhibited graphically by the appearance of negative coefficients. Despite these defects, *all* of the polynomials reproduce numerical coefficients for an independently calculated value of τ to within the accuracy of the original computer program.

Almost all of our series analysis (Sec. II C) takes the form of extrapolations in (βJ) at fixed, numerical values of $(\beta\Delta)$. There is, of course, no difficulty in rearranging (2.4), (2.6), or (2.7) as true high-*temperature* expansions, $\sum_{n=0}^{\infty} c_n(J/\Delta) \times(\beta\Delta)^n$; however, the series so obtained are empirically quite poorly behaved in the vicinity of the TCP. This probably reflects the fact that (i) the Taylor expansion of τ in powers of $\beta\Delta$ has a radius of convergence of only $[\pi^2+(\ln 2)^2]^{1/2}$ and (ii) the slope $|dT_c(\Delta)/d\Delta|$ is large near the TCP (Sec. III C), so a path $T \to T_c(\Delta)^+$ at constant Δ is close to being tangent to the critical line and spends a long time in the critical region.

B. Derivation of low-temperature-series coefficients

Low-temperature finite-field expansions for the $s=\frac{1}{2}$ Ising model have been derived by the King's College group,[42–45] using strong lattice constants tabulated by Sykes *et al.*[44,46] The procedure for $s>\frac{1}{2}$ is complicated by the appearance of multiple bonds but has been carried through by Fox, Gaunt, and Guttmann[47] for $s=1$ and $\frac{3}{2}$, and extended to general spin by Saul and Ferer.[48]

Our derivation of the Blume-Capel series follows the lines of Ref. 47 but uses a new trick[48] to simplify the multiple-bond problem. Consider two distinguishable types of particles with occupation numbers $n_1(1)$ and $n_2(1)$, respectively, at site 1. Suppose each lattice site can be occupied by at most one particle, so $n_1(1)+n_2(1)=0,1$. Rewrite the spin variable $S(1)=1-n_1(1)-2n_2(1)$. When the Hamiltonian (1.1) is reexpressed in terms of n_1 and n_2, the partition function becomes

$$Z(\beta J,\beta\Delta,\beta h)=e^{\beta N(qJ/2-\Delta)}\sum_{\{n_1(1),n_2(1)\}}(u^q\mu\eta)^{\sum_1 n_1(1)}(u^q\mu)^{2\sum_1 n_2(1)}u^{\sum_{\langle 12\rangle}[n_1(1)n_1(2)+2n_1(1)n_2(2)+2n_2(1)n_1(2)+4n_2(1)n_2(2)]}, \tag{2.10}$$

where $\mu\equiv e^{-\beta h}$, $\eta\equiv e^{\beta\Delta}$, $u\equiv e^{-\beta J}$, N is the number of sites on the lattice, and $\sum_{\{n_1(1),n_2(1)\}}$ denotes the sum over all occupations. The ground state of the system (at $h=0$) is the particle vacuum, provided $\Delta<\frac{1}{2}qJ$. Each term in the sum corresponds to a point cluster G of occupied sites (disconnected clusters *are* included) and contributes a "weight"

$$w[G]=(u^q\mu\eta)^{N_1}(u^q\mu)^{2N_2}u^{-B[G]}, \tag{2.11}$$

where N_1 and N_2 are, respectively, the number of type-1 and -2 particles in the cluster G and

$$B[G]=b_{11}[G]+2b_{12}[G]+4b_{22}[G], \tag{2.12}$$

with $b_{ij}[G]$ the number of i-j nearest-neighbor bonds in G. Each cluster occurs many times on the lattice; however, because of the extensivity of the free energy,[42] it is only that term in the occurrence which is linear in N which survives in $-\beta f=\ln Z/N$. Thus,

$$-\beta f(\beta J,\beta\Delta,\beta h)=\tfrac{1}{2}qJ+h-\Delta+\sum_G m[G]w[G], \tag{2.13}$$

where the multiplicity[48] $m[G]$ is related to the strong lattice constants[44,46] $[G]$ by

$$m[G]=[G]g[\overline{G}]/g[G]. \tag{2.14}$$

$g[G]$ and $g[\overline{G}]$ are the symmetry factors[33,34] of the original cluster G (with type-1 and type-2 particles distinguished) and the "reduced" cluster $\overline{G}$ in which the distinction between particle types is suppressed. Figure 1 gives two examples.

It is convenient to collect powers of μ and to

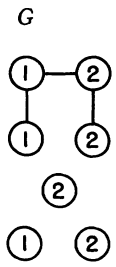

G	$w[G]$	$m[G]$
	$(u^{12}\mu\eta)^2(u^{12}\mu)^4u^{-7}$	$282\left(\frac{2}{1}\right)=564$
	$(u^{12}\mu\eta)(u^{12}\mu)^4$	$70\frac{1}{3}\left(\frac{3!}{2!}\right)=211$

FIG. 1. Examples of contributions to the low-temperature free-energy series for the fcc Blume-Capel model. Low-temperature lattice constants are taken from Appendix IV of Ref. 42.

write the result

$$-\beta f(\beta J,\beta\Delta,\beta h)=\tfrac{1}{2}qJ+h-\Delta+\sum_{n=1}^{\infty}(u^{12}\mu)^n L_n(u,\eta)\,, \tag{2.15}$$

where $L_n(u,\eta)=\sum_{m=0}^{n}L_{nm}(u)\,\eta^m$ is a polynomial in u^{-1} and η. $L_{nm}=0$ unless n and m are both even or both odd. The lattice constants necessary for $n\leq 5$ have been published by Sykes, Essam, and Gaunt.[44] The six-point clusters appear first in $L_{66}(u)$, where they are decorated only with type-1 particles. Such contributions can be taken quite generally from the $s=\frac{1}{2}$ Ising polynomials given in Ref. 44 with $u^{6n}L_{nn}(u)=[L_n(u)]_{\text{Sykes}}$. The fcc Blume-Capel polynomials L_n, $1\leq n\leq 6$, are given in Table II. For $\Delta=-\infty$, $\eta=0$, they reduce correctly to the $s=\frac{1}{2}$ Ising results.[44] For $\Delta=0$, $\eta=1$, they are in precise agreement with the $s=1$ polynomials.[47]

All thermodynamic information can be derived from (2.15) by appropriate differentiation. We do not have low-temperature correlation-function data such as contained in (2.7). Series analysis is normally done at $h=0$ ($\mu=1$). For a fixed, numerical value of $\beta\Delta$, (2.15) (and corresponding expansions for other quantities) is a series in ascending powers of u, which can be analyzed by standard methods.

C. Analysis of series

Table III gives definitions and expected asymptotic singular behavior of the quantities for which we have analyzed series. Our notation for the critical indices conforms, in general, to that of Riedel.[11,15,16] Analysis was done at $h=0$ along paths of constant $\beta\Delta$, i.e., along straight lines passing through the origin in the T,Δ phase diagram, Fig. 2. The quantity x is the spin analog of the fractional He^3 concentration in He^3-He^4 mixtures[1,14] and is called the "nonordering density" by Riedel.[11] We shall denote high- and low-temperature versions of a typical exponent θ by θ and θ', respectively. θ_u and θ_t will denote tricritical exponents along paths respectively parallel and at finite angle to the phase boundary.[11–13] If tricritical scaling holds, then $\theta_u=\theta_t/\varphi_t$, where φ_t is the crossover exponent.

The quantities with specific-heat-like indices deserve special mention, since they seem to exhibit somewhat anomalous behavior for $T\geq T_c$ ($\beta\Delta$) (Sec. IV A). C_Δ is related to the fluctuations of the local energy density,[49]

$$k_BT^2NC_\Delta=\langle(\mathcal{H}-\langle\mathcal{H}\rangle)^2\rangle\ . \tag{2.16}$$

When $h=0$, the right-hand side has three terms [see (1.1)]: The first is the fluctuations of the exchange energy $-J\sum_{\langle 12\rangle}S^z(1)S^z(2)$, the third is the fluctuations of the anisotropy energy $\Delta\sum_1[S^z(1)]^2$, and the second is twice the cross fluctuations. The third term is just $N\Delta^2Y$. $k_BT^2NC_{\beta\Delta}$ is the first plus half of the cross term. Scaling suggests that all three terms should diverge similarly in the critical region, and we expect $\alpha_\Delta=\alpha_{\beta\Delta}=\lambda=1-\omega\equiv\alpha$. Such behavior is, indeed, observed away from T_t; however, near the TCP at $T>T_c$ the amplitudes of the direct and cross fluctuations have opposite signs and appear to become nearly equal

TABLE II. Low-temperature free-energy polynomials for the fcc Blume-Capel model. See Eq. (2.15).

$$L_{11}(u)=1$$

$$L_{20}(u)=1$$

$$L_{22}(u)=\frac{13}{2}+\frac{6}{u}$$

$$L_{31}(u)=-13+\frac{12}{u^2}$$

$$L_{33}(u)=\frac{211}{3}-\frac{120}{u}+\frac{42}{u^2}+\frac{8}{u^3}$$

$$L_{40}(u)=-\frac{13}{2}+\frac{6}{u^4}$$

$$L_{42}(u)=211-\frac{120}{u}-\frac{240}{u^2}+\frac{84}{u^3}+\frac{42}{u^4}+\frac{24}{u^5}$$

$$L_{44}(u)=-944\tfrac{1}{4}+\frac{2322}{u}-\frac{1653}{u^2}+\frac{126}{u^3}+\frac{123}{u^4}+\frac{24}{u^5}+\frac{2}{u^6}$$

$$L_{51}(u)=211-\frac{240}{u^2}-\frac{78}{u^4}+\frac{84}{u^6}+\frac{24}{u^8}$$

$$L_{53}(u)=-3777+\frac{4644}{u}+\frac{3522}{u^2}-\frac{4568}{u^3}-\frac{426}{u^4}+\frac{84}{u^5}+\frac{296}{u^6}+\frac{168}{u^7}+\frac{48}{u^8}+\frac{8}{u^9}$$

$$L_{55}(u)=14303\tfrac{1}{5}-\frac{45792}{u}+\frac{49290}{u^2}-\frac{16296}{u^3}-\frac{2871}{u^4}+\frac{792}{u^5}+\frac{448}{u^6}+\frac{96}{u^7}+\frac{30}{u^8}$$

$$L_{60}(u)=\frac{211}{3}-\frac{120}{u^4}+\frac{42}{u^8}+\frac{8}{u^{12}}$$

$$L_{62}(u)=-5665\tfrac{1}{2}+\frac{2322}{u}+\frac{9288}{u^2}-\frac{2244}{u^3}-\frac{2046}{u^4}-\frac{1248}{u^5}-\frac{1680}{u^6}+\frac{804}{u^7}-\frac{180}{u^8}+\frac{276}{u^9}+\frac{240}{u^{10}}+\frac{96}{u^{11}}+\frac{24}{u^{12}}+\frac{12}{u^{13}}$$

$$L_{64}(u)=71516-\frac{137376}{u}-\frac{17010}{u^2}+\frac{144356}{u^3}-\frac{40758}{u^4}-\frac{17280}{u^5}-\frac{5914}{u^6}-\frac{708}{u^7}+\frac{1521}{u^8}+\frac{952}{u^9}+\frac{480}{u^{10}}+\frac{168}{u^{11}}+\frac{54}{u^{12}}$$

$$L_{66}(u)=-234103\tfrac{1}{6}+\frac{922152}{u}-\frac{1329240}{u^2}+\frac{771272}{u^3}-\frac{64224}{u^4}-\frac{65070}{u^5}-\frac{6904}{u^6}+\frac{3930}{u^7}+\frac{1212}{u^8}+\frac{776}{u^9}+\frac{168}{u^{10}}+\frac{30}{u^{11}}+\frac{1}{u^{12}}$$

in magnitude. The resulting cancellation makes α_Δ and $\alpha_{\beta\Delta}$ difficult to observe.

Most of our series analysis was done by now-standard techniques.[50–52] In the determination of high-temperature exponents and amplitudes we have (with one exception noted below) relied on direct ratio analysis of the series coefficients. If the quantity to be analyzed

$$Q=\sum_{n=0}^{\infty} c_n (\beta J)^n \sim A t^{-\theta} \tag{2.17}$$

($t \equiv 1 - T_c/T$), then the ratios of successive coefficients go asymptotically for large n as

$$\rho_n \equiv \frac{c_n}{c_{n-1}} \sim \frac{k_B T_c}{J}\left(1+\frac{\theta-1}{n}\right) . \tag{2.18}$$

Neville-table extrapolation of ρ_n gives estimates of $k_B T_c/J$. When θ is known or can be guessed with confidence, the approximants $n\rho_n/(n+\theta-1)$ converge to kT_c/J more rapidly than ρ_n. Conversely, when T_c is known, $(Jn\rho_n/k_B T_c - n + 1)$ converges rapidly to θ. For given T_c and θ, the amplitude A can be found by Neville extrapolation of the approximants $c_n (J/k_B T_c)^n/\binom{n+\theta-1}{n}$. Results of the above methods were often corroborated by logarithmic derivative series and Padé methods.

The part of the second-order line near the tricritical point presents special problems. Universality predicts that the critical indices are Δ independent (i.e., remain rigorously Ising-like) right up to the TCP and then cross over[53] discontinuously to their tricritical values. Furthermore, even at $\Delta = 0$ ($s = 1$ Ising), the ratios (2.18) plotted against $1/n$ are significantly curved compared with $\Delta = -\infty$ ($s = \frac{1}{2}$ Ising), in a way which is not removed by Neville extrapolation and indicates the presence of a confluent singularity as a correction to leading scaling behavior.[54–57] To incorporate these features—universality, confluency, and crossover—we hypothesize [cf. (2.18)]

$$Q \sim A t^{-\theta} + B t^{-\theta+\epsilon} \tag{2.19}$$

at $t \to 0$. In the fully second-order region ϵ determines the strength of the confluent singularity. At the TCP, $\theta_t = \theta - \epsilon$, $A = 0$, and the tricritical amplitude $A^{(t)} \equiv B$. The asymptotic expression for ρ_n which follows from (2.19) is more complicated than (2.18). With θ now assumed known, each c_n may be expressed in terms of the four parameters, T_c, A, B, and ϵ. Conversely, each set of four successive coefficients, c_n c_{n+1}, c_{n+2}, and c_{n+3}, produces estimates $(T_c)_n$, A_n, B_n, and ϵ_n. In favorable cases these estimates converge smoothly and rapidly (Sec. IV B). We refer to this as the "four-fit" technique.

It is well known from work on the Ising model[58] that the low-temperature series typically possess singularities in the complex u plane closer to the origin than the physical singularity u_c. Ratio techniques are, therefore, inapplicable, and at low temperatures we have relied exclusively on Padé methods.[50–51] If $Q \sim A(u_c - u)^{-\theta}$, then Padés of the log derivative $d/du \ln Q$ have a pole at $u = u_c$ with residue θ. Furthermore, Padé approximants to the series $(u_c - u)Q^{1/\theta}$ may be evaluated at $u = u_c$ to obtain estimates of $A^{1/\theta}$. Where data are available, we have generally taken u_c to be determined from the high-temperature evaluation of T_c.

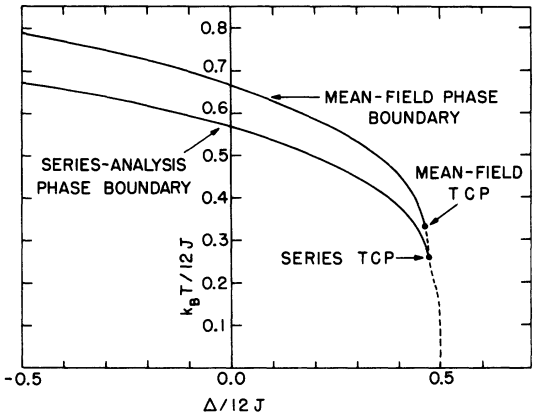

FIG. 2. $T_c(\Delta)$ phase diagram. Mean-field results are plotted for comparison. Second-order and first-order parts of the phase boundary are shown as full and dashed lines, respectively. Below the series TCP, mean-field and series first-order phase boundaries are indistinguishable on this scale.

TABLE III. Definitions and expected singular behavior of quantities for which series were analyzed. All analysis except the critical isotherm data (involving δ) was done at $h = 0$ along paths of constant $\beta\Delta$. $t \equiv |1 - T_c(\beta\Delta)/T|$.

Definition	Singular behavior
$\chi_0 = -\dfrac{\partial^2 f}{\partial h^2}$	$k_B T \chi_0 \sim A_\chi t^{-\gamma}$
μ_2 [see (2.7)]	$\mu_2 \sim A_\mu t^{-(\gamma+2\nu)}$
$M = \langle S(1)\rangle = -\dfrac{\partial f}{\partial h}$	$M \sim A_M t^{\beta}$
	$\beta h \sim A_\delta M^{\delta}$ $(T = T_c)$
$\mathfrak{L} = -\dfrac{\partial^4 (\beta f)}{\partial (\beta h)^4}$	$\mathfrak{L} \sim A_{\mathfrak{L}} t^{-(\gamma+2\Delta)}$
$x = 1 - \langle S^2(1)\rangle = 1 - \dfrac{\partial f}{\partial \Delta}$	$x \sim x_c \pm A_x t^{\omega}$ $(T \gtrless T_c)$
$\beta Y = \dfrac{\partial x}{\partial \Delta} = -\dfrac{\partial^2 f}{\partial \Delta^2}$	$Y \sim A_Y t^{-\lambda}$
$C_\Delta = \dfrac{T}{N}\dfrac{\partial S}{\partial T}\Big\|_\Delta$	$\dfrac{C_\Delta}{k_B} \sim A_\Delta t^{-\alpha_\Delta}$
$C_{\beta\Delta} = \dfrac{T}{N}\dfrac{\partial S}{\partial T}\Big\|_{\beta\Delta}$	$\dfrac{C_{\beta\Delta}}{k_B} \sim A_{\beta\Delta} t^{-\alpha_{\beta\Delta}}$

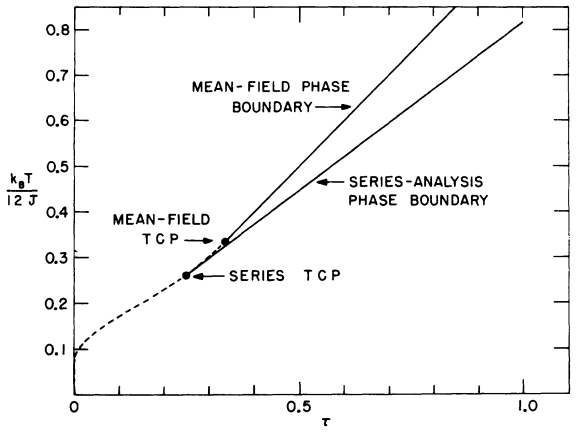

FIG. 3. $T_c(\tau)$ phase diagram. $\tau \equiv (1+\frac{1}{2}e^{\beta\Delta})^{-1}$. Mean-field results are plotted for comparison. Second-order and first-order parts of the phase boundary are shown as full and dashed lines, respectively. For small τ the mean-field first-order boundary becomes indistinguishable from series results on this scale.

III. $h=0$ PHASE DIAGRAM

A. Overview

The computed $T_c(\Delta)$, $T_c(\tau)$, and $T_c(x)$ phase diagrams are shown as Figs. 2–4. Second- and first-order phase boundaries are shown as full and dashed lines, respectively. Mean-field results[14] are plotted for comparison. Figures 5 and 6 show $T_c(\Delta)$ and $T_c(x)$ data in detail in the vicinity of the TCP and will be discussed in Secs. III C and IV C. Phase-diagram data are available in tabular form.[59]

The parameters of the tricritical point are

$$\begin{aligned} &\tau_t = 0.248 \pm 0.010, \qquad (\beta\Delta)_t = 1.80 \pm 0.05, \\ &k_B T_t/12J = 0.2615 \pm 0.0070, \\ &\Delta_t/12J = 0.4716 \pm 0.0010, \\ &x_t = 0.665^{+0.005}_{-0.015}. \end{aligned} \tag{3.1}$$

Determination of τ_t is discussed in Sec. III C. The temperature T_t is marginally higher than previously quoted[24] (see Sec. III C). The uncertainty in $k_B T_c/12J$ at a fixed value of τ near τ_t is only about ± 0.001. The larger uncertainty quoted reflects the uncertainty in the actual value of τ_t. A similar comment applies to Δ_t, but the corresponding uncertainty is smaller because of the steep slope of $T_c(\Delta)$ near the TCP. The determination of x_t involves an additional extrapolation to find x at fixed $\tau = \tau_t$ and $T = T_t$ from high- or low-temperature series (Sec. IV B and IV C) and is accordingly rather crude.

The principal features of the phase diagram are as follows: (i) The mean-field phase diagram is qualitatively correct; however, as expected, mean-field transition temperatures are uniformly high. (ii) The slope of the phase boundary across the TCP appears finite and continuous in both $T_c(\tau)$ and $T_c(\Delta)$. (iii) The three branches of the phase boundary in $T_c(x)$ appear to be linear near the TCP and to have unequal slopes. (iv) The slope $-dT_c(\Delta)/d\Delta$ is not monotonically increasing with Δ; the phase boundary $T_c(\Delta)$is concave upward in a small region just below the TCP.

Points (ii)–(iv) are in agreement with mean-field theory, except that the two high-temperature branches of $T_c(x)$ have equal slope in mean-field theory. The data plotted in Fig. 6 make clear that the evidence for point (iii) is comparatively weak: The high-temperature data, while quite linear, show only a small discontinuity in slope at the TCP[60]; the low-temperature extrapolations are so crude (Sec. IV C) as to provide little more than the suggestion that T_c is only weakly dependent on x for $0.4 < x < x_t$. Point (iv) is in disagreement with the best He^3-He^4 data of Behringer, Goellner, and Meyer.[4]

We divide our data into three regions: the fully second-order region ($1.0 > \tau > 0.3$), the tricritical region ($0.3 > \tau > 0.2$), and the fully first-order region ($0.2 > \tau > 0.0$). In the second-order region we have relied for phase-diagram determination on ratio estimates of $T_c(\tau)$ from susceptibility series (2.6), using the Ising value $\gamma = \frac{5}{4}$. These series are extremely well behaved and we put uncertainties at one part in 10^3 or better. Ratio values are confirmed by four-fit analysis (Sec. II C). This part of the phase diagram has previously been studied by Oitmaa.[25–27] His values of T_c are slightly higher than ours near the TCP, a discrepancy which we

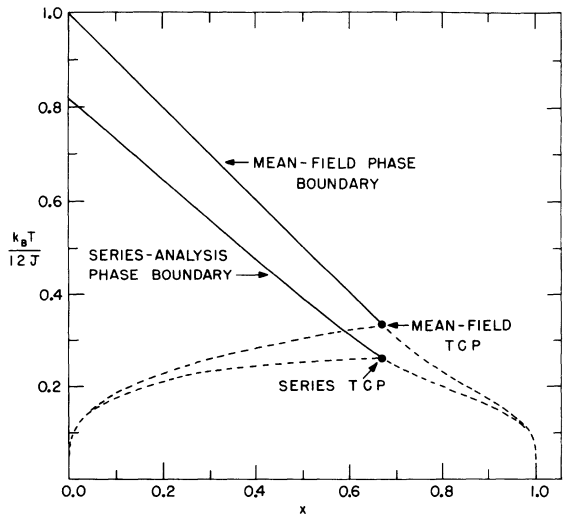

FIG. 4. $T_c(x)$ phase diagram. Mean-field results are plotted for comparison. Second-order and first-order parts of the phase boundary are shown as full and dashed lines, respectively.

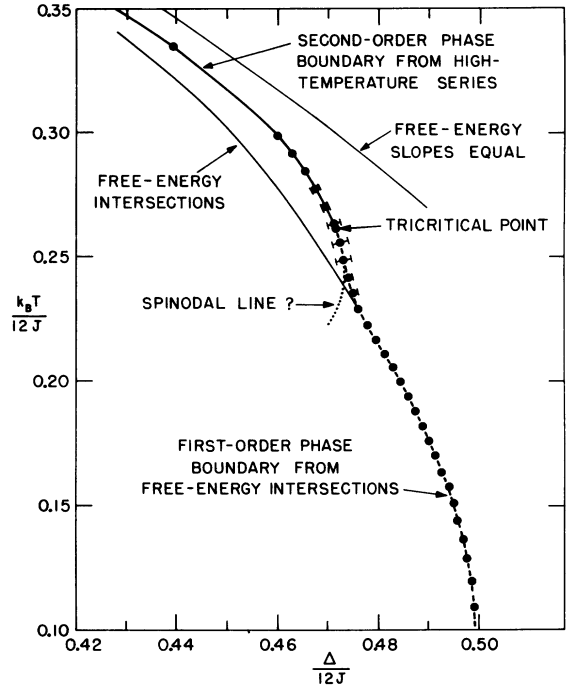

FIG. 5. $T_c(\Delta)$ phase diagram; detail near the tricritical point. Unless shown explicitly, uncertainties are smaller than plotted points. In addition to the phase-boundary curve, the spinodal line (dotted) from high-temperature series and the free-energy intercepts and points of equal slope (light lines) are shown. See text.

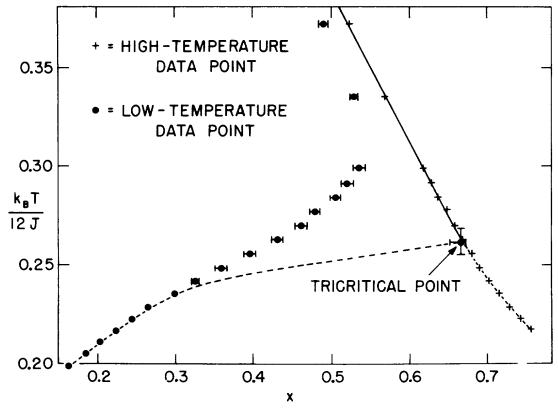

FIG. 6. $T_c(x)$ phase diagram; detail near the tricritical point. Series data, given as points, show apparent extrapolation uncertainties. Lines are our best estimate of correct phase boundaries. High- and low-temperature data should (but do not) agree at and above the tricritical point. High-temperature data are the more reliable, when the two disagree. See Sec. IV C and Ref. 79.

attribute to his shorter series (seven terms in χ_0 as opposed to our 12) and his use of γ values appreciably less than $\frac{5}{4}$.

The discussion of the first-order and tricritical regions is presented in Secs. III B and III C below.

B. Free-energy intersection and the location of the first-order phase boundary

Quantities such as χ_0, which are strongly divergent at second-order transitions, are believed for Ising-like models to exhibit at most a very weak (essential) singularity on approach to a first-order boundary.[61,62] Conventional series methods for locating a second-order transition are, therefore, inapplicable to a first-order transition. The method we use depends on the fact that the free energy has discontinuous first derivatives at a first-order transition. At a second-order transition it is, of course, second derivatives which are divergent.

Our procedure consists in extrapolating the $h=0$ high- and low-temperature free-energy series (2.4) and (2.15) at fixed values of $\beta\Delta$. Extrapolation is carried out simply by evaluating diagonal and near-diagonal Padé approximants to $-\beta f$, using the variables βJ at high temperatures and u at low temperatures. We have also tried direct extrapolation of the partial sums in (2.4), a line which gives almost identical results. Figure 7 shows some typical plots. For $\beta\Delta \gg (\beta\Delta)_t$ there is

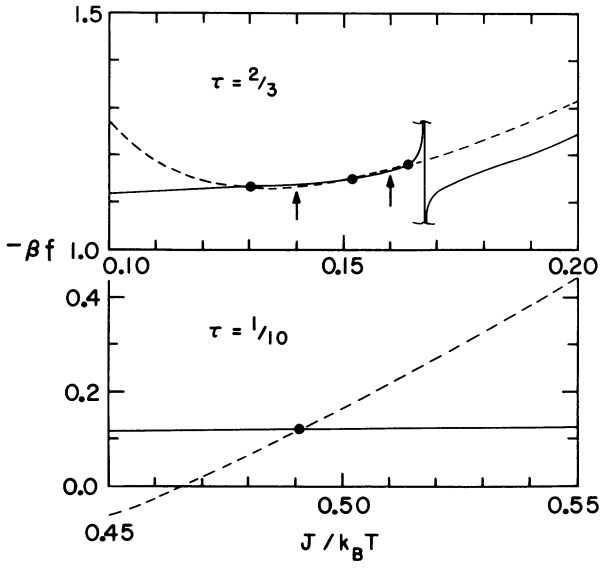

FIG. 7. Typical free-energy-intersection curves for the first- ($\tau=\frac{1}{10}$) and second- ($\tau=\frac{2}{3}$) order regions. τ is defined by (2.2). The solid curves plot the high-temperature [7, 6] Padé approximant. The dashed curves plot the low-temperature [33, 33] Padé approximant. Points of intersection and equal slope are marked by heavy dots and arrows, respectively. Note that the peculiar behavior of the $\tau=\frac{2}{3}$ [7, 6] Padé takes place at $J/k_BT=0.167$, well beyond the range of validity of the high-temperature series.

a single, well-defined intersection of the high- and low-temperature free-energy curves (with the correct limiting behavior near $T=0$, $\Delta=6J$), which we identify with the first-order transition. Because of the essential singularity mentioned above,[61] it is a moot point whether or not the *true* high- and low-temperature free-energy functions possess analytic extensions beyond the first-order phase boundary. Our finite-series approximants do not, of course, contain such singularities, though they do have a variety of real poles and zeros beyond the intersections, which may or may not indicate a spinodal line.[62] In the fully first-order region the dominant uncertainty comes from the low-temperature series, and we have found transition temperatures by calculating the intercepts of successive low-temperature Padés with the (7, 6) high-temperature Padé. The estimated uncertainty in the transition temperature is as large as $\frac{1}{2}\%$ at $\tau=0.2$ but decreases rapidly with τ and is smaller than one part in 10^4 below $\tau=0.1$.

The free-energy intersection method is also applicable in the fully second-order region, though as a determinant of T_c it is appreciably less precise than the method described in Sec. III A. Its importance at high temperatures lies in the fact that it is the only method which spans the tricritical point. By comparing it in the second-order region with the more precise $k_BT\chi_0$ method, a judgment of its accuracy may be made. The $\tau=\frac{2}{3}$ ($\Delta=0$, $s=1$ Ising) curves shown in Fig. 7 are typical of this region and illustrate the inherent difficulties. Rigorously speaking, the high- and low-temperature free-energy functions should meet and have a common tangent at T_c. Finite-series extrapolants do not, of course, meet exactly, and there is difficulty in finding an *a priori* criterion for locating T_c. By following the behavior of the approximants from the first-order region, one can argue that it is the middle one of the three intercepts which is physical. Nearby, at a slightly higher temperature, the slopes of the two free-energy approximants are equal. Empirically one finds that the average position of the intercept and the point of equal slope agrees with the susceptibility-based critical temperature to better than $\frac{1}{2}\%$ throughout the fully second-order region.[63] Note, in addition, that the *true* free energy has infinite curvature at the critical point. Finite-term series cannot mimic such behavior, and it is perhaps not surprising that there is an "overshoot" which carries the point of equal slope away from the intercept. For $\tau=\frac{2}{3}$, depicted in Fig. 7, we find $J/k_BT=0.152$ (intercept), 0.140 (equal slope), and 0.147 (χ_0 series). Both the high- and low-temperature series are less well converged in the second-order region than in the first-order region, and the apparent uncertainty in the intercept itself is as much as 2%.

C. Phase boundary in the tricritical region and the location of the TCP

The vicinity $0.2<\tau<0.3$ of the tricritical point is depicted in Fig. 5. Our phase boundary follows the $k_BT\chi_0$ critical temperature (Sec. III A) down to $\tau=0.25$ ($k_BT/12J=0.263$). Beyond this we interpret the critical temperatures from the four-fit analysis (which also appear in standard ratio analysis[26]) as at best tracing out a spinodal curve or at worst being entirely a figment of too-short series. On the first-order side the phase boundary follows the free-energy intercept (Sec. III B) up to $\tau=0.21$ ($k_BT/12J=0.235$). Beyond this the intercept is, we believe, below the phase boundary because of the overshoot mentioned above. Both first- and second-order boundaries develop appreciable uncertainties near the TCP. For $0.21<\tau<0.25$ the phase boundary shown in Fig. 5—which we take henceforth as standard—is a smooth curve joining the first- and second-order regions and drawn through the upper edge of the envelope of uncertainty.

Our data cannot strictly rule out the possibility that the true phase boundary follows the $k_BT\chi_0$ and intercept curves right up to their intersection at $k_BT/12J=0.239$, $\Delta/12J=0.473$. This would, however, put the TCP a good deal below our preferred position. Moreover, it would make the slope of the $T_c(\Delta)$ phase boundary discontinuous across the TCP. Such a discontinuity is not seen in He^3-He^4 mixtures[3,4] and is not easily reconciled with present theories of tricritical behavior.

Despite the large uncertainties in the phase boundary near the TCP (±0.002 in $\Delta/12J$), two observations can be made with some confidence: (i) The concavity of the $T_c(\Delta)$ phase boundary [point (iv) of Sec. III A] is real. Note that the existence of the dip is already established well outside the uncertain region $0.23<k_BT_c/12J<0.27$. (Such a dip is found for $d=2$ by Monte Carlo calculations.[28]) (ii) The point of vertical tangency, $dT_c(\Delta)/d\Delta \to -\infty$, of the four-fit $T_c(k_BT_c/12J=0.242)$ is very close to the intercept curve in a region where the intercepts are expected to be below the correct phase boundary and, therefore, is *not* a likely candidate for the TCP.[64]

Having fixed now the position of the phase boundary, we turn to the location of the TCP, itself. The methods given so far locate the TCP only crudely. Approaching from the second-order side, one expects the relatively well-determined susceptibility index to retain its universal Ising value, $\gamma=\frac{5}{4}$, right up to the TCP. Finite-series effects make this a poor criterion for choosing the TCP, since direct ratio estimates show γ smoothly decreasing from $\tau=0.4$, and already by the time $\tau=0.3$, $\gamma\approx1.12$. Taking the point of vertical tan-

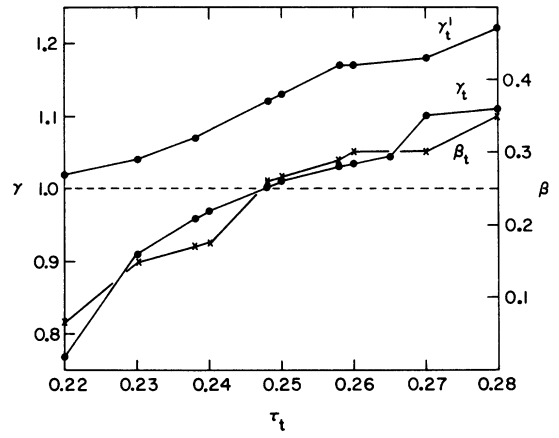

FIG. 8. Dependence of the effective tricritical exponents on the choice of the TCP τ_t. τ is defined by (2.2). Reading uncertainties in γ_t and γ_t' are ± 0.01, while those in β_t are ± 0.02. The dotted line shows mean-field tricritical values.

gency as the lower limit, one can only conclude $0.22 < \tau_t < 0.30$. On the other hand, the free-energy intersections should develop a continuous slope as the TCP is approached from the first-order side. With finite series, the discontinuity never disappears entirely, although it first vanishes *to within extrapolation uncertainties* in the region $0.23 < \tau < 0.26$. To fix the tricritical point more precisely we are forced to use secondary methods.

Direct reading of ratio estimates and Padé tables (Sec. IV A) for $0.23 \leq \tau \leq 0.26$ gives (see Fig. 8) $0.91 \leq \gamma \leq 1.03$, $1.04 \leq \gamma' \leq 1.17$, and $0.15 \leq \beta \leq 0.30$. These values are notably consistent with the Landau tricritical exponents $\gamma_t = \gamma_t' = 1$, $\beta_t = \frac{1}{4}$, which also agree (logarithmic corrections aside) with the renormalization-group calculation of Riedel and Wegner.[15,16] Assuming that any one of these exponents is valid provides a criterion for picking τ_t. Referring to Fig. 8, we choose the value (3.1) for τ_t

Alternately, we may study the behavior of the critical amplitudes A_χ and A_μ defined in Table III. If tricritical scaling[11-13,53] holds, then near the TCP A_χ should vanish as $(\tau - \tau_t)^{(\gamma-\gamma_t)/\varphi_t} = (\tau - \tau_t)^{1/2}$ (using[15,16] $\gamma_t = 1$, $\varphi_t = \frac{1}{2}$). Similarly, A_μ should vanish as $(\tau - \tau_t)^{1.03 \pm 0.03}$, where the uncertainty allows $0.625 \leq \nu \leq 0.638$[39,65] with[15,16] $\nu_t = \frac{1}{2}$. Figure 9 shows A_χ and A_μ as determined from four-fits (Sec. IV B). This consideration suggests a value of τ_t slightly higher than (3.1); however, we consider it somewhat less reliable because of the difficulty of getting good amplitudes.

IV. EXPONENTS AND AMPLITUDES

On the basis of the phase diagram constructed in Sec. III, we now summarize our results for indices and amplitudes.[66] We discuss in turn the tricritical region (Riedel's[11] region III), the second-order or critical region (Riedel's region II), and the first-order region (Riedel's region I).

A. Tricritical region

Table IV tabulates our tricritical results. In these determinations the position of the TCP (τ_t, T_t) is regarded as input data. We have relied on ratio methods above T_t and on Padé log derivatives below, as outlined in Sec. II C. The sources of uncertainty are (i) apparent reading uncertainties of Neville or Padé tables, (ii) discrepancies in the determination of the same quantity by two or more different methods, e.g., the high-temperature A_χ and A_μ may be studied by ratios or identified as the coefficient B in the four-fit (2.19) (these uncertainties are not quoted; however, see Ref. a, Table IV), (iii) uncertainties in the location of the TCP, and finally for amplitudes only (iv) uncertainty in the assumed value of the tricritical exponent (these uncertainties are not quoted; however, see Refs. b and i, Table IV). The most important source of uncertainty is usually (iii), though the others can also be appreciable, especially for amplitudes. Figure 8 illustrates the dependence of some typical exponents on the assumed location of the TCP along the standard phase boundary. We have *not* tried to place *over-all confidence limits* on the numbers in Table IV.

Bausch[19] has argued on the basis of the Ginzburg criterion that tricritical exponents should be mean-field-like for dimensionality $d > 3$. By analogy with ordinary critical phenomena, where mean-field theory holds for $d > 4$ and there are logarithmic corrections at $d = 4$, one might expect logarithmic corrections to tricritical mean-field theory at $d = 3$. The calculations of Riedel and Wegner[15-17] support these expectations. (Historically Ref. 15 predates

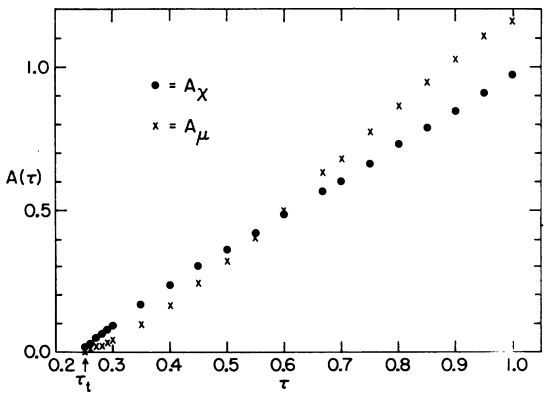

FIG. 9. Critical amplitudes $A_\chi(\tau)$ and $A_\mu(\tau)$, as determined from four-fits to high-temperature series. Uncertainties are shown on Fig. 10.

TABLE IV. Tricritical exponents and amplitudes. See Table III for definitions. Analysis is done at the TCP (3.1). Mean-field tricritical exponents are shown for comparison. In determining amplitudes we have, unless otherwise noted, used observed tricritical exponents at high temperatures and the mean-field tricritical exponents at low temperatures. We quote apparent reading uncertainties in Neville and Padé tables. The two lower numbers demonstrate the variations as T_t ranges over its uncertainty $0.238 \leq \tau_t \leq 0.258$.

Quantity	Tricritical exponent	High temperature	Low temperature	Mean-field tricritical exponent	Tricritical amplitude	High temperature	Low temperature
		1.00 ± 0.01	1.12 ± 0.01			0.241 ± 0.001[a]	0.04152 ± 0.00001[b]
χ_0	γ_t	0.96 1.03	1.07 1.17	1	$A_\chi^{(t)}$	0.210 0.276	0.0408 0.0425
		0.505 ± 0.008				0.221 ± 0.005[a]	
μ_2	ν_t	0.49 0.54	c	$\frac{1}{2}$	$A_\mu^{(t)}$	0.18 0.27	c
			0.26 ± 0.02				1.68 ± 0.02
M	β_t	d	0.17 0.29	$\frac{1}{4}$	$A_M^{(t)}$	d	1.59 1.79
			5.2 ± 0.5				0.43 ± 0.01
M	δ_t[e]	d	4.5 6.3	5	$A_\delta^{(t)}$	d	0.33 0.52
			1.29 ± 0.01				0.00702 ± 0.00002
$\mathfrak{L}$	Δ_t	c	1.23 1.34	$\frac{5}{4}$	$A_{\mathfrak{L}}(t)$	c	0.0069 0.0073
		0.55 ± 0.05				2.10 ± 0.02	
x	ω_t	0.52 0.55	*f*	$\frac{1}{2}$	$A_x^{(t)}$	2.00 2.22	*f*
		0.47 ± 0.04				0.505 ± 0.005	
Y	λ_t	0.47 0.48	$0.7^{+0.4}_{-0.2}$[g]	$\frac{1}{2}$	$A_Y^{(t)}$	0.48 0.52	*f*
			0.599 ± 0.001				1.86 ± 0.02[i,j]
C_Δ	$(\alpha_{\beta\Delta})_t$	-0.6 ± 0.03[g]	0.59 0.60	$\frac{1}{2}$	$A_\Delta^{(t)}$	0.39 ± 0.05[g,h]	1.14 1.22
			0.609 ± 0.001				1.253 ± 0.001[j]
$C_{\beta\Delta}$	$(\alpha_{\beta\Delta})_t$	k	0.60 0.61	$\frac{1}{2}$	$A_{\beta\Delta}^{(t)}$	k	0.120 1.29

[a]Amplitude was determined by ratio method (Neville table). Four-fits give $A_\chi^{(t)} = 0.22 \pm 0.02$, $A_\mu^{(t)} = 0.21 \pm 0.01$.
[b]Uses $\gamma_t' = 1.12$. The mean-field value $\gamma_t' = 1$ gives $A_\chi^{(t)\prime} = 0.0654 \pm 0.0005$ (0.0532, 0.0787).
[c]Not obtainable from our series.
[d]Not defined.
[e]For method, see D. S. Gaunt, Proc. Phys. Soc. Lond. 92, 150 (1967).
[f]Padé estimates not converged.
[g]Series estimates very poorly converged; order of magnitude only.
[h]Uses $(\alpha_\Delta)_t = -0.5$.
[i]Uses observed exponents $(\alpha_\Delta')_t = (\alpha_{\beta\Delta}')_t = 0.6$. Extrapolants are less well behaved with $(\alpha_\Delta')_t = (\alpha_{\beta\Delta}')_t = 0.5$: They give, for example, $A_\Delta^{(t)} = 1.9 \pm 0.2$ (1.7, 2.3).
[j]Note the maximum in the $A_\Delta^{(t)}$ calculated with $(\alpha_\Delta')_t = 0.6$.
[k]Series is poorly converged and appears dominated by a singularity well below T_t. See text.

Ref. 19.) With the exception of the poorly behaved high-temperature specific-heat data, *our tricritical exponents agree with tricritical mean-field theory*. We have not attempted to analyze for possible logarithmic corrections.[67]

The high-temperature tricritical specific-heat index is crudely consistent with $(\alpha_\Delta)_t = -\frac{1}{2}$ and well below the strong, mean-field divergence[68] $(\alpha_\Delta)_t = (\alpha_{\beta\Delta})_t = \frac{1}{2}$. The fact that the related exponents (Table III) $1-\omega_t \approx \lambda_t \approx \frac{1}{2}$ suggests that there is a cancellation or near cancellation of the leading high-temperature tricritical singularity of C_Δ. A careful look at the tricritical behavior of the three terms in C_Δ discussed after (2.16) confirms this suspicion: All three diverge separately as $t^{-1/2}$. The first and third are equal but are canceled by the cross fluctuations to within uncertainties. The tricritical ratios (2.18) of the series coefficients belonging to $C_{\beta\Delta}$ show an even more dramatic behavior: They should asymptotically rise to $k_B T_t/J = 3.138$; instead, they decrease monotonically after $n=7$ and $\rho_{11}=1.40$, suggesting that our short series miss the tricritical singularity altogether and are dominated by a singularity at a much lower temperature.

There is a simple scaling argument which correlates both these observations with the steep slope $|dT_c/d\Delta|$ near the TCP. *If* this slope were infinite at the TCP, then we could identify the scaling fields[69] $\mu_1 \sim \Delta - \Delta_t$ and $\mu_2 \sim T - T_t$. The scaling Ansatz for the free energy is

$$-\beta f(\mu_1, \mu_2) = \mu_1^{2-\alpha_t} \mathcal{F}(\mu_2/\mu_1^{\varphi_t})$$

[where $\mathcal{F}(x)$ denotes *some* function of the variable x, *not* generally the same function from one usage to the next] so the entropy would go as

$$s = \frac{\partial f}{\partial t} \sim \frac{\partial f}{\partial \mu_2} \sim \mu_1^{2-\alpha_t-\varphi_t} \mathcal{F}\left(\frac{\mu_2}{\mu_1^{\varphi_t}}\right) .$$

Thus,

$$C_\Delta \sim \frac{\partial^2 f}{\partial \mu_2^2} \sim \mu_1^{2-\alpha_t-2\varphi_t} \mathcal{F}\left(\frac{\mu_2}{\mu_1^{\varphi_t}}\right) , \tag{4.1}$$

while $C_{\beta\Delta}$ would have a term going as

$$C_{\beta\Delta} \sim \frac{\partial^2 f}{\partial \mu_1 \partial \mu_2} \sim \mu_1^{1-\alpha_t-\varphi_t} \mathcal{F}\left(\frac{\mu_2}{\mu_1^{\varphi_t}}\right) . \tag{4.2}$$

Assuming mean-field tricritical indices, $\alpha_t = \varphi_t = \frac{1}{2}$, we would observe along the tricritical path $\tau = \tau_t$

$$C_\Delta \sim t^{1/2}, \quad C_{\beta\Delta} \sim t^0 + t^{1/2}, \tag{4.3}$$

while in the second-order region[70]

$$C_\Delta \sim (\tau - \tau_t)^{5/4} t^{-1/8}, \quad C_{\beta\Delta} \sim (\tau - \tau_t)^{1/4} t^{-1/8}. \tag{4.4}$$

The behavior (4.3) is in agreement with our observations. We believe, however, that the actual slope of the phase boundary at the TCP is large but finite (Sec. III C). We hypothesize, therefore, that the cancellation, while good enough to "fool" the high-temperature series, is actually incomplete. There seems to be no theoretical reason why a vertical tangent of $T_c(\Delta)$ should be a general feature of the TCP. If, for example, a term $-K\sum_{\langle 12\rangle} S^2(1) S^2(2)$ were added[14,71] to the Blume-Capel Hamiltonian, one would expect the tricritical slope of $T_c(\Delta)$ to be K dependent. This understanding of the high-temperature specific-heat anomaly is, of course, speculative and leaves moot the question of why the low-temperature specific heat appears normal.

There is another example of the effect of the steepness of $T_c(\Delta)$ near the TCP. We have done a direct ratio analysis of the susceptibility series at constant $\Delta/J = \Delta_t/J$ (see Sec. II A). These series are quite poor but give crudely $\chi_0 \sim (T - T_t)^{-1.85\pm0.40}$. This appears inconsistent with $\gamma_t = 1$, since scaling predicts the same exponent for all paths at a finite angle to the phase boundary. The explanation is that near the TCP $\chi_0 \sim \mu_1^{-\gamma_t} \mathcal{F}(\mu_2/\mu_1^{\varphi_t}) \sim \mu_2^{-\gamma_t/\varphi_t} \mathcal{F}(\mu_1^{\varphi_t}/\mu_2)$. For a phase boundary vertical at the TCP, $\mu_1 = 0$ along $\Delta = \Delta_t$ and $\chi_0 \sim t^{-2}$, where we have used mean-field tricritical indices.

B. Critical region and the cross-over exponent φ_t

We study in this section the behavior of the amplitudes A (Table III) along the second-order phase boundary ($\tau > \tau_t$). In contrast to some previous work,[25-27] we assume the validity of universality in feeling free to set all exponents equal to their Ising-like values[72] for any $\tau > \tau_t$. The results of four-fit analysis (Sec. II C) for the high-temperature amplitudes $A_\chi(\tau)$ and $A_\mu(\tau)$ are shown in Fig. 9. ϵ values for χ_0 remain within ± 0.1 of the apparently universal[54-57] value $\epsilon \approx \frac{1}{2}$ for $\tau > 0.37$. Below this they cross over smoothly (presumably because of finite-series effects) to $\epsilon \approx \frac{1}{4}$ at $\tau = \tau_t$. For $\tau \geq 0.45$ ratio and four-fit amplitudes A_χ are within 3% agreement. Below, ratio amplitudes are progressively higher and do not vanish at T_t.[73]

Both A_χ and A_μ are well determined and remarkably linear[74] for $0.3 < \tau < 1.0$. Below $\tau = 0.3$ uncertainties are appreciable; however, vanishing of the amplitudes at the TCP (3.1) clearly requires curvature in the region $\tau_t < \tau < 0.3$. Figure 10 shows the same data plotted against $(\tau - \tau_t)$ on a log-log scale. Tricritical scaling[11,12] predicts the "amplitude scaling" relations

$$\chi_0 \sim (\tau - \tau_t)^{(\gamma-\gamma_t)/\varphi_t} t^{-\gamma},$$
$$\mu_2 \sim (\tau - \tau_t)^{(\gamma+2\nu-\gamma_t-2\nu_t)/\varphi_t} t^{-(\gamma+2\nu)} \tag{4.5}$$

near the TCP but in the second-order region. There are large uncertainties, but in $\tau_t \leq \tau \leq 0.3$ the data for both A_χ and A_μ are compatible with $0.27 \leq \varphi_t \leq 0.62$. The mean-field exponent φ_t

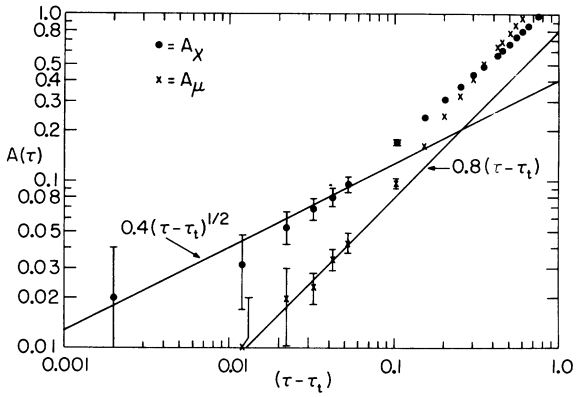

FIG. 10. Log-log plots of high-temperature amplitudes $A_\chi(\tau)$ and $A_\mu(\tau)$ versus $(\tau-\tau_t)$, showing apparent reading uncertainties. The straight lines show the fits (4.7) to the data near the TCP.

$=\frac{1}{2}$ falls in this range, and we quote

$$\varphi_t = 0.5^{+0.1}_{-0.2}. \tag{4.6}$$

With the crossover exponent now fixed at $\varphi_t=\frac{1}{2}$, we find for $\tau_t<\tau<0.33$

$$A_\chi(\tau)=0.4(\tau-\tau_t)^{1/2},\quad A_\mu(\tau)=0.8(\tau-\tau_t), \tag{4.7}$$

as shown in Fig. 10.

Series for the other amplitudes are not sufficiently regular to support four-fit analysis, which clearly separates out the coefficient of $t^{-\theta}$, even for τ near τ_t. Other methods of amplitude determination tend to see a single "effective" singularity and, thus, cross over smoothly between critical and tricritical behavior. The difficulty is illustrated by the magnetization amplitude $A_M(\tau)$ shown in Fig. 11. The Padé analysis uses the Ising exponent $\beta=\frac{5}{16}$ and a T_c determined from high-temperature susceptibility series. Beyond $\tau=0.3$ the series have switched over to the tricritical exponent $\beta_t=\frac{1}{4}$ and the approximants to A_M systematically fail to converge.[73] Tricritical scaling predicts $A_M \sim (\tau-\tau_t)^{(\beta_t-\beta)/\varphi_t}=(\tau-\tau_t)^{-1/8}$. The series amplitudes decrease as τ decreases and seem at first glance to be in disagreement. Actually the coefficient in the proportionality can also be predicted by invoking two-scale-factor universality.[75-77] A_χ and A_μ fix the scales (n and g) and we deduce

$$\frac{A_M(\tau)}{A_M(1)}=\frac{[A_\chi(\tau)/A_\chi(1)]^{5/4}}{[A_\mu(\tau)/A_\mu(1)]^{3/4}}\quad; \tag{4.8}$$

so, using (4.7) and the $s=\frac{1}{2}$ data from Table V, $A_M(\tau)=0.64(\tau-\tau_t)^{-1/8}$ in the tricritical region, as plotted on Fig. 11. Considering the crudeness of (4.7), agreement is not bad [changing the constants in (4.7) to 0.5 and 0.7 improves things a lot].

Expressions of universality such as (4.8) should also hold away from the tricritical point. The discrepancy between the measured and predicted $A_M(\tau)$ (see Fig. 11)—which constitutes an apparent violation of two-scale-factor universality—is harder to explain for $\tau\gtrsim 0.4$, where the amplitudes $A_\chi(\tau)$ and $A_\mu(\tau)$ have much smaller apparent uncertainties. Consider the relatively well-studied $s=1$ Ising series ($\tau=\frac{2}{3}$). Our amplitudes, given in Table V, agree well with values quoted by other workers; yet, the discrepancy in Fig. 11 is 13%. An even more direct test of universality is the equality of the high- and low-temperature susceptibility ratios,

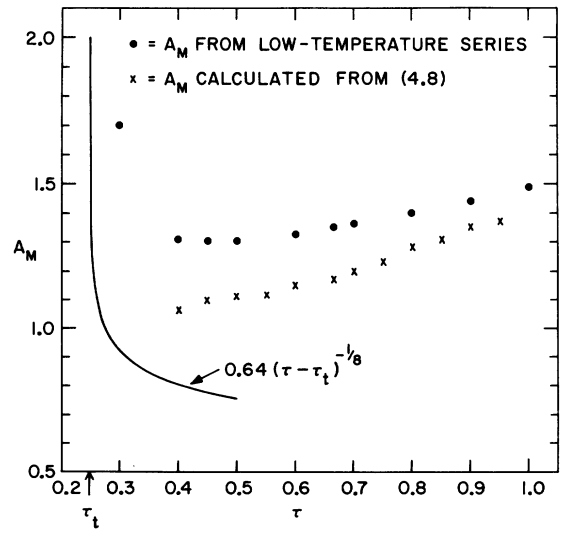

FIG. 11. Critical magnetization amplitude $A_M(\tau)$. Dots show data from series analysis (Padés). Crosses show $A_M(\tau)$ as calculated via universality, Eq. (4.8). The solid curve shows the tricritical region, as calculated from (4.7) and (4.8).

TABLE V. Selected amplitudes for $s=\frac{1}{2}$ and $s=1$ fcc Ising models ($\tau=1$, $\frac{2}{3}$). $s=1$ numbers are from our $\tau=\frac{2}{3}$ Blume-Capel data (other references given) and carries apparent reading uncertainties only.

	$s=\frac{1}{2}$	$s=1$
A_χ	0.9750 ± 0.0003[a]	0.565 ± 0.005[b]
A_μ	1.137 ± 0.001[a]	0.631 ± 0.002
A_M	1.4869 ± 0.0018[c]	1.350 ± 0.006[d]
A'_χ	0.1892 ± 0.0002[c]	0.1273 ± 0.0002[d]
A_δ	0.375 ± 0.010[e]	0.868 ± 0.010[f]

[a]Reference 77.

[b]Reference 75 quotes $\frac{3}{2}A_\chi=C_2^*=0.877$, which seems rather too high.

[c]J. M. Essam and D. L. Hunter, J. Phys. C 1, 392 (1968).

[d]Reference 48 quotes $A_M=1.361\pm0.001$ and $A'_\chi=0.739\pm0.053$ on the basis of series somewhat longer than ours.

[e]D. S. Gaunt, Proc. Phys. Soc. Lond. 92, 150 (1967).

[f]Reference 47 quotes $A_\delta=0.84\pm0.05$ on the basis of series somewhat longer than ours.

$$\frac{A_\chi(\tau)}{A_\chi(1)}=\frac{A_\chi'(\tau)}{A_\chi'(1)}\,. \tag{4.9}$$

For $\tau=\frac{2}{3}$ our data give 0.579 and 0.673 for the left- and right-hand sides, respectively. Similarly, universality predicts

$$\frac{A_s(1)}{A_s(\tau)}=\frac{A_\chi(\tau)}{A_\chi(1)}\left[\frac{A_M(\tau)}{A_M(1)}\right]^4, \tag{4.10}$$

and for $\tau=\frac{2}{3}$ our data give 0.432 and 0.394. Either there is a real failure of universality or some amplitudes with good apparent convergence are actually in error by as much as 10%. Both possibilities are distasteful; however, we tend to opt for the second. Amplitudes are exceedingly sensitive to nearby and/or confluent singularities.

C. First-order region

According to scaling[11] a quantity Q which goes as $Q\sim\mu_1^{-\theta_t}\mathcal{F}(\mu_2/\mu_1^{\varphi_t})$ near the TCP should behave along the first-order phase boundary ($\mu_1=0$) as $Q\sim\mu_2^{-\theta_u}\sim(\tau_t-\tau)^{-\theta_u}$ with $\theta_u=\theta_t/\varphi_t$. For $\tau<\tau_t$ all thermodynamic quantities are for practical purposes (see Sec. III B) nonsingular on approach to the (first-order) phase boundary. To calculate the value of Q at the boundary, we have simply formed the Padé approximants to Q and evaluated them at the appropriate transition temperature.[78] High-temperature series are apparently quite well converged even for small values of τ, for which the transition temperature approaches zero. Low-temperature series are comparatively poorly converged except for $\tau<0.22$.

Figures 4 and 6 illustrate our data for the concentration x in the first-order region. The high-temperature data are linear in the vicinity of the TCP and appear to suffer a small but distinct discontinuity in slope[60] [point (iii) in Sec. III A]. Taking $\omega_u=1$ from the linearity of the phase boundary, we compute $\varphi_t=\omega_t/\omega_u=0.5$ in confirmation of (4.6). The low-temperature data, on the other hand, are very poor above $x=0.3$ ($\tau=0.21$): At the tricritical temperature low-temperature extrapolation gives $x=0.42$ (cf. $x=0.665$ from above). Above the TCP, where high- and low-temperature determinations of x should coincide, the low-temperature data continue to rise to a maximum of $x=0.54$ (at $\tau=0.30$) but remain always well below the high-temperature data.[79] Disturbingly, the *apparent* uncertainty in the low-temperature extrapolations (Fig. 6) is entirely insufficient to reconcile them with the high-temperature data, which we regard as reliable. Between $x=0.3$ and the TCP the low-temperature phase boundary in Fig. 6 is no more than a well-informed sketch.

Figure 12 shows the magnetization M_u just below the phase boundary in the first-order region. According to scaling M_u should vanish as[80] $(\tau_t-\tau)^{\beta_u}$ with $\beta_u=\frac{1}{2}$. The observed slope gives $\beta_u\approx0.2$ ($\approx\beta_t$). Apparently the low-temperature series, poorly converged near the TCP, are unable to follow the rapid decrease of the magnetization at fixed τ, as T approaches the phase boundary from below.[81] Thus, the series data never really penetrates into Riedel's[11] region I, and we are inclined to regard the observed slope in Fig. 12 as evidence *in favor* of $\beta_t=\frac{1}{4}$ rather than against $\beta_u=\frac{1}{2}$.

V. CONCLUSIONS

Our results are almost entirely in agreement with the mean-field, Riedel-Wegner,[15,16] scaling[11–13] picture of a $d=3$ tricritical point. In particular, (a) we find a phase diagram (Figs. 2–6) in which $T_c(\Delta)$ is linear near the TCP and has continuous slope, while $T_c(x)$ is linear but has discontinuous slope. (b) Tricritical exponents are symmetric and agree with the mean-field, Riedel-Wegner indices ($\gamma_t=1,\nu_t=\alpha_t=\frac{1}{2},\beta_t=\frac{1}{4}$, etc.) with the sole (and explainable) exception of the high-temperature specific heat. We have not tried to analyze for logarithmic factors.[17] (c) Critical amplitudes become singular as the TCP is approached from the second-order side with exponents which are compatible with tricritical scaling and a crossover exponent $\varphi_t=\frac{1}{2}$.

Various other theories are not compatible with our results. Reatto's droplet model[82] gives a susceptibility amplitude near the second-order phase boundary which is independent of the distance from the TCP, in disagreement with (4.7) and Figs. 9 and 10. Stauffer's modified version[83] predicts $\gamma_t=\frac{2}{3}$, in disagreement with our $\gamma_t=1$. Kortman's theory[84] predicts a susceptibility amplitude which vanishes as $(\Delta_t-\Delta)^{\gamma-1}=(\Delta_t-\Delta)^{1/4}$, in disagreement with (4.7). We have been unable to compare our results with the theory of Rice and Chang.[85]

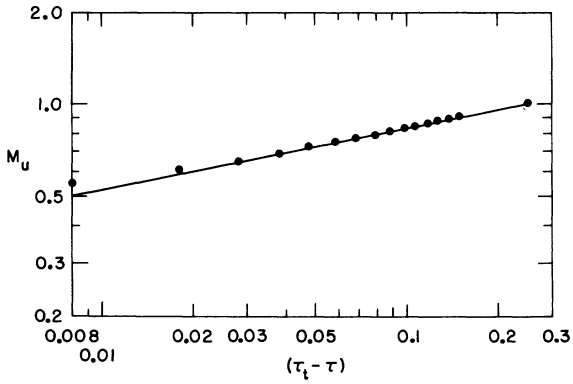

FIG. 12. Magnetization at the first-order phase boundary. Data points are from Padé extrapolation of low-temperature series. The slope at $\tau\to\tau_t^-$ should give the first-order index β_u. See text for discussion.

How do results for other models compare with ours? Harbus and Stanley[30] recently used high-temperature series to study a metamagnetic system with competing in-plane and out-of-plane interactions. They found a tricritical susceptibility divergence $\chi_{\text{meta}} \sim t^{-1/2}$, a result corroborated by Arora and Landau using Monte Carlo methods.[28] The magnetization in the metamagnet is the non-ordering density, so their χ_{meta} is the analog of our Y and their result agrees with our $\lambda_t = \frac{1}{2}$. However, not all models studied have shown mean-field-like tricritical exponents. Arora and Landau[28] find (Monte Carlo) for the $d=2$ Blume-Capel model $\gamma_t = 1.1 \pm 0.4$, $\gamma_t' = 1.0 \pm 0.3$, but $\beta_t = 0.09 \pm 0.02$ and $\delta_t = 10.8 \pm 0.7$. This is perhaps not surprising, since it is well known that critical indices are d dependent and, more specifically, the Ginzburg criterion[19] suggests that for $d=2$ the Blume-Capel tricritical point is fluctuation dominated (Sec. I). More provocatively, a $d=3$ Ising model with competing nn and nnn interactions, studied by Harbus and Stanley,[31] and by Landau[86] shows $\lambda_t = \frac{1}{4}$ and $\omega_t = 0.78 \pm 0.20$. These data seem to require the existence of a non-mean-field-like TCP in $d=3$, i.e., a non-Gaussian tricritical fixed point.

Is there more than one type of tricritical point in $d=3$? The experimental data are still inconclusive: He^3-He^4 seems mean-field-like[3,4]; however, both DAG[6-8] and $FeCl_2$[9,10] show strong indications of non-mean-field exponents. This nice question remains open, pending further and more definitive work.

ACKNOWLEDGMENTS

We thank M. Blume and R. B. Griffiths for initially drawing our attention to this problem. We acknowledge with pleasure useful communications with G. Ahlers, B. L. Arora, R. Bausch, M. Blume, R. B. Griffiths, A. Hankey, F. Harbus, R. Krasnow, D. P. Landau, H. Meyer, and particularly, E. K. Riedel.

---

*Research supported in part by the National Science Foundation under Grant No. NSF-GP-40395.

[1]R. B. Griffiths, Phys. Rev. Lett. 24, 715 (1970).
[2]E. H. Graf, D. M. Lee, and J. D. Reppy, Phys. Rev. Lett. 19, 417 (1967).
[3]G. Ahlers, in *The Physics of Liquid and Solid Helium*, edited by J. B. Ketterson and K. H. Bennemann (Wiley, New York, 1974), Chap. 8.
[4]G. Goellner and H. Meyer, Phys. Rev. Lett. 25, 1534 (1971); G. Goellner, R. Behringer, and H. Meyer, J. Low Temp. Phys. 13, 113 (1973); E. Riedel, H. Meyer, R. Behringer, and G. Goellner (unpublished). References 3 and 4 contain many additional references.
[5]W. B. Yelon, in Proceedings of the NATO A.S.I., 1973 (unpublished); W. B. Yelon, D. E. Cox, P. J. Kortman, and W. B. Daniels, Phys. Rev. B (to be published).
[6]D. P. Landau, B. E. Keen, B. Schneider, and W. P. Wolf, Phys. Rev. B 3, 2310 (1971); W. P. Wolf, B. Schneider, D. P. Landau, and B. E. Keen, Phys. Rev. B 5, 4472 (1972).
[7]G. F. Tuthill, F. Harbus, and H. E. Stanley, Phys. Rev. Lett. 31, 527 (1973).
[8]R. Alben, W. P. Wolf, and A. T. Skjeltorp (unpublished).
[9]I. S. Jacobs and P. E. Lawrence, Phys. Rev. 164, 866 (1967); R. J. Birgeneau, W. B. Yelon, E. Cohen, and J. Makovsky, Phys. Rev. B 5, 2607 (1972); W. B. Yelon and R. J. Birgeneau, Phys. Rev. B 5, 2615 (1972).
[10]R. J. Birgeneau, G. Shirane, M. Blume, and W. C. Koehler (private communication).
[11]E. K. Riedel, Phys. Rev. Lett. 28, 675 (1972).
[12]A. Hankey, H. E. Stanley, and T. S. Chang, Phys. Rev. Lett. 29, 278 (1972).
[13]R. B. Griffiths, Phys. Rev. B 7, 545 (1973).
[14]M. Blume, V. J. Emery, and R. B. Griffiths, Phys. Rev. A 4, 1071 (1971). The original discussion of tricritical mean-field theory was given by L. D. Landau, Phys. Z. Sowjetunion 11, 26 (1937), reprinted in *Collected Papers of L. D. Landau*, edited by D. ter Haar (Pergamon, London, 1965), p. 193. The BEG model is discussed in a cluster-variation approximation by W. M. Ng, J. H. Barry, and T. Tanaka, in *Proceedings of the 13th International Conference on Low-Temperature Physics* (University of Colorado, to be published).
[15]E. K. Riedel and F. J. Wegner, Phys. Rev. Lett. 29, 349 (1972).
[16]E. K. Riedel, AIP Conf. Proc. 10, 865 (1973).
[17]F. J. Wegner and E. K. Riedel, Phys. Rev. B 7, 248 (1973).
[18]E. K. Riedel and F. J. Wegner, Phys. Rev. B 9, 294 (1974).
[19]R. Bausch, Z. Phys. 254, 81 (1972). Bausch's argument shows that mean-field theory is self-consistent (but not necessarily correct) at $d > 3$.
[20]L. P. Kadanoff *et al.*, Rev. Mod. Phys. 39, 395 (1967).
[21]M. Blume, Phys. Rev. 141, 517 (1966).
[22]H. W. Capel, Physica (Utr.) 32, 966 (1966); 33, 295 (1967); 37, 423 (1967).
[23]The full T, Δ, h phase diagram has three critical lines meeting at the TCP. See Ref. 14.
[24]D. M. Saul and M. Wortis, AIP Conf. Proc. 5, 349 (1972).
[25]J. Oitmaa, Phys. Lett. A 33, 230 (1970).
[26]J. Oitmaa, J. Phys. C 4, 2466 (1971).
[27]J. Oitmaa, J. Phys. C 5, 435 (1972).
[28]B. L. Arora and D. P. Landau, AIP Conf. Proc. 10, 870 (1973).
[29]D. P. Landau (private communication).
[30]F. Harbus and H. E. Stanley, Phys. Rev. Lett. 29, 58 (1972); Phys. Rev. B 8, 1141 (1973).
[31]F. Harbus and H. E. Stanley, Phys. Rev. B 8, 1156 (1973).
[32]F. Englert, Phys. Rev. 129, 567 (1963).
[33]M. Wortis, D. Jasnow, and M. A. Moore, Phys. Rev. 185, 805 (1969).
[34]M. Wortis, in *Phase Transitions and Critical Phenomena*, edited by C. Domb and M. S. Green (Academic, New York, 1974), Vol. 3.
[35]*Handbook of Mathematical Functions*, edited by M. Abramowitz and I. A. Stegun (National Bureau of Stan-

dards, Washington, D. C., 1964), Eq. 3.6.24.

[36]The calculation which we outline below for the free energy can be carried through in an entirely analogous way for the susceptibility and second moment (2.6) and (2.7).

[37]The contribution of the two-point graph with n edges is $\frac{1}{2}q(M_n^0)^2(\beta J)^n/n!$.

[38]We chose the (closed-packed) fcc lattice for our study because fcc series lack antiferromagnetic singularities and are appreciably more regular to given order in n than corresponding series on the sc or bcc lattices.

[39]M. A. Moore, D. Jasnow, and M. Wortis, Phys. Rev. Lett. 22, 940 (1969).

[40]This involves summing linked-cluster graphs with two, three, and four vertices. In a similar way we have calculated the τ^2 and τ^3 coefficients in $m_n^{(0)}$ and $m_n^{(2)}$.

[41]Comparison of our series with the $s=\frac{1}{2}$ Ising ($\tau=1$) data of the King's College group reveals a slight discrepancy.

[42]C. Domb, Adv. Phys. 9, 149 (1960).

[43]*Phase Transitions and Critical Phenomena*, edited by C. Domb and M. S. Green (Academic, New York, 1974), Vol. 3.

[44]M. F. Sykes, J. W. Essam, and D. S. Gaunt, J. Math. Phys. 6, 283 (1965).

[45]M. F. Sykes *et al.*, J. Math. 14, 1060 (1973); 14, 1066 (1973); 14, 1071 (1973).

[46]M. F. Sykes, J. W. Essam, B. R. Heap, and B. J. Hiley, J. Math. Phys. 7, 1557 (1966).

[47]P. F. Fox and D. S. Gaunt, J. Phys. C 3, L88 (1970); 5, 3085 (1972). P. F. Fox and A. J. Guttmann, Phys. Lett. A 31, 234 (1970); J. Phys. C 6, 913 (1973); A. J. Guttmann (private communication). See also M. F. Sykes and D. S. Gaunt, J. Phys. A 6, 643 (1973).

[48]D. Saul and M. Ferer (unpublished).

[49]K. Huang, *Statistical Mechanics* (Wiley-Interscience, New York, 1963).

[50]D. S. Gaunt and A. J. Guttmann, in Ref. 43.

[51]D. L. Hunter and G. A. Baker, Jr., Phys. Rev. B 7, 3346 (1973); 7, 3377 (1973).

[52]D. Jasnow and M. Wortis, Phys. Rev. 176, 739 (1968).

[53]E. K. Riedel and F. Wegner, Z. Phys. 225, 195 (1969).

[54]M. Wortis, Newport Beach Conference on Phase Transitions, 1970 (unpublished).

[55]F. Wegner, Phys. Rev. B 5, 4529 (1971).

[56]M. A. Moore, D. M. Saul, and M. Wortis, J. Phys. C (to be published); D. M. Saul and M. Wortis (unpublished).

[57]E. Brézin, J. C. Le Guillou, and J. Zinn-Justin, Saclay Report No. DPH T Lecture 73 24, 1973 (unpublished).

[58]C. Domb and A. J. Guttmann, J. Phys. C 3, 1652 (1970).

[59]D. M. Saul, Ph.D. thesis (University of Illinois, 1974) (unpublished).

[60]A continuous slope with a large second derivative in the T, x plane near the TCP cannot be strictly ruled out by series-extrapolation evidence.

[61]M. E. Fisher, Physics 3, 255 (1967); J. S. Langer, Ann. Phys. (N. Y.) 41, 108 (1967).

[62]See, for example, K. Binder and E. Stoll, Phys. Rev. Lett. 31, 47 (1973).

[63]The low-temperature Padés to $-\beta f$ are monotonic increasing with order (along the diagonal), a trend which we have not tried to extrapolate in drawing Fig. 5. It is clear from Fig. 7 that a modest (and entirely conceivable) increase could bring the high- and low-temperature curves into tangency at a properly intermediate T_c.

[64]In Ref. 26 Oitmaa used the vertical tangent to locate his TCP at $k_BT_t/12J\approx 0.27$. In Ref. 27 he uses his second-order phase boundary (higher than ours, see Sec. III A) and a presumed variational property of mean-field theory to conclude $k_BT_t/12J\geq 0.296$. Notice that both Oitmaa, Refs. 25–27, and Harbus and Stanley, Refs. 30 and 31, lack low-temperature series and, therefore, have data only in the second-order region.

[65]M. E. Fisher and R. J. Burford, Phys. Rev. 156, 583 (1967).

[66]More complete data are available in Ref. 59.

[67]Our data are simply not clean enough to sustain systematic introduction of the possibility of logarithms into the analysis. Crudely speaking, however, $\ln t$ looks like a small negative power. Following these lines is *not* always encouraging. For example, Riedel and Wegner, Refs. 15–17, predict $M\sim(|t|\ln|t|)^{1/4}$ at the TCP, which might be expected to show up in series analysis as an effective β_t slightly less than 0.25. This is not observed.

[68]Actually, in strict mean-field theory all nonanalyticities in T derivatives of the free energy come via the order parameter, which vanishes at $h=0$, $T>T_c$, so *strictly* $(\alpha_\Delta)_t=(\alpha_{\beta\Delta})_t=0$ [even though $(\alpha'_\Delta)_t=(\alpha'_{\beta\Delta})_t=\frac{1}{2}$]. This special and unphysical situation is restricted to $h=0$ and disappears entirely in the calculation of Ref. 15–17, where fluctuations are correctly incorporated. We quote the symmetrical exponents.

[69]Our notation follows Ref. 11. μ_2 and μ_1 measure distance, respectively, along and at finite angle to the phase boundary.

[70]Note that the second-order amplitudes vanish as $\tau\to\tau_t$. This is in marked contrast to the behavior of

$$Y\sim\frac{\partial^2 f}{\partial\mu_1^2}\sim(\tau-\tau_t)^{-3/4}t^{-1/8}$$

in the second-order region. In a similar vein, the Pippard relations [M. J. Buckingham and W. M. Fairbank, in *Progress in Low-Temperature Physics*, edited by C. J. Gorter (North Holland, Amsterdam, 1961), Vol. III, Chap. 3] give

$$\frac{1}{T}\frac{\partial E}{\partial T}\bigg|_\Delta=\frac{C_\Delta}{T}=\left(\frac{d\Delta}{dT_c}\right)^2\frac{\partial x}{\partial\Delta}\bigg|_T\ ,$$

so C_Δ is down by a factor $|d\Delta/dT_c|^2$ relative to Y. We can, in fact, observe (Ref. 59) A_Y growing as $\tau\to\tau_t^+$, while A_Δ and $A_{\beta\Delta}$ are difficult to isolate but seem to decrease.

[71]F. Rys, Helv. Phys. Acta 42, 606 (1969); 42, 608 (1969); J. Bernasconi and F. Rys. Phys. Rev. B 4, 3045 (1971).

[72]This index universality is consistent with direct analysis of the series except in the near vicinity of $\tau=\tau_t$.

[73]If the proper *effective* index is used at each τ, the ratio amplitude goes over smoothly to the (finite) tricritical amplitude $A^{(t)}$. If the critical exponent is rigidly fixed at θ, when the series is becoming tricritical (θ_t), the amplitude approximants are not well-converged.

[74]It is at first tempting to suppose that A_χ remains linear right down to the TCP. This would put the TCP near $\tau=0.21$, unacceptably lower than (3.1). If it were possible to maintain τ_t at (3.1), a linear A_χ would require $\varphi_t=\frac{1}{4}$. This is inconsistent with a linear phase boundary $T_c(x)$ (by scaling) and is the opposite to the direction

necessary for resolving $\beta_t \approx \beta_u$ (Sec. IV C). Footnote 18 of Ref. 31 was based on a premature interpretation of this linear trend.

[75]D. D. Betts, A. J. Guttmann, and G. S. Joyce, J. Phys. C 4, 1994 (1971).

[76]D. Stauffer, M. Ferer, and M. Wortis, Phys. Rev. Lett. 29, 345 (1972); M. Ferer, D. Stauffer, and M. Wortis, AIP Conf. Proc. 10, 836 (1973).

[77]M. Ferer and M. Wortis, Phys. Rev. B 6, 3426 (1972).

[78]We have also tried forming Padés to quantities like $Q^{1/\theta}$, with θ some appropriately chosen tricritical or spindoal index. Results do not differ significantly.

[79]In the Ising $s=\frac{1}{2}$ limit $x=0$ rigorously, and T_c is known quite precisely. Even with the greater length of low-temperature series available (Ref. 44), we find at $T=T_c$ *by Padé extrapolation* $x=0.01$, with apparent uncertainties which exclude $x=0$. The diagonal and near-diagonal x Padés (see also Ref. 63) for $\tau \geq 0.22$ *do* show a monotonic increasing trend. Presumably this slow trend continues and, given a sufficient number of terms, brings x up to its high-temperature value for $\tau > \tau_t$; however, with the number of terms available to us, realistic extrapolation of the trend is hopeless.

[80]Note that our index β_u is equivalent to Griffiths' s (Ref. 13) ζ_u. Griffiths's β_u measures the behavior of a metamagnet's magnetization in the first-order region, a quantity which is the analog of our x.

[81]Analogously, the low-temperature x series is unable to follow the rapid *increase* in concentration as the first-order phase boundary is approached near the TCP from below.

[82]L. Reatto, Phys. Rev. B 5, 204 (1972).

[83]D. Stauffer, Phys. Rev. B 6, 1839 (1972).

[84]P. R. Kortman, Phys. Rev. Lett. 29, 1449 (1972). A_χ is determined only crudely by Fig. 10, and the rest of Kortman's exponents are actually quite close to ours.

[85]O. K. Rice and Do-Ren Chang, Phys. Rev. A 5, 1419 (1972).

[86]D. P. Landau, Phys. Rev. Lett. 28, 449 (1972); see also R. F. Altman, S. Spooner, and D. P. Landau, AIP Conf. Proc. 10, 1163 (1973).